Supplementary Material

1 SUPPLEMENTARY TABLES AND FIGURES

1.1 Figures

1.1.1 Wind Noise

We account for the lack of in-situ wind conditions using both model-based (AVO-G2S) and data-based (leveraging onset times between CLES and CLCO) methods to calculate the effective sound speed for each explosion (c_{eff}). We chose to use the data-based method for subsequent analyses in the study because we feel that it may incorporate the changes in atmospheric conditions the best.

To further investigate the effect of wind, we follow the methods of Fee and Garces (2007) for looking at the low frequency (0.02-0.3 Hz) component of infrasound for each explosion. However, this type of analysis shows essentially the "magnitude of noise", whereas the c_{eff} calculations that we are interested in also account for directionality of the wind conditions. We show the power spectral density (PSD) for the 60 minutes of CLES infrasound data prior to each explosion using 60 s windows with 50% overlap (Figure S1).

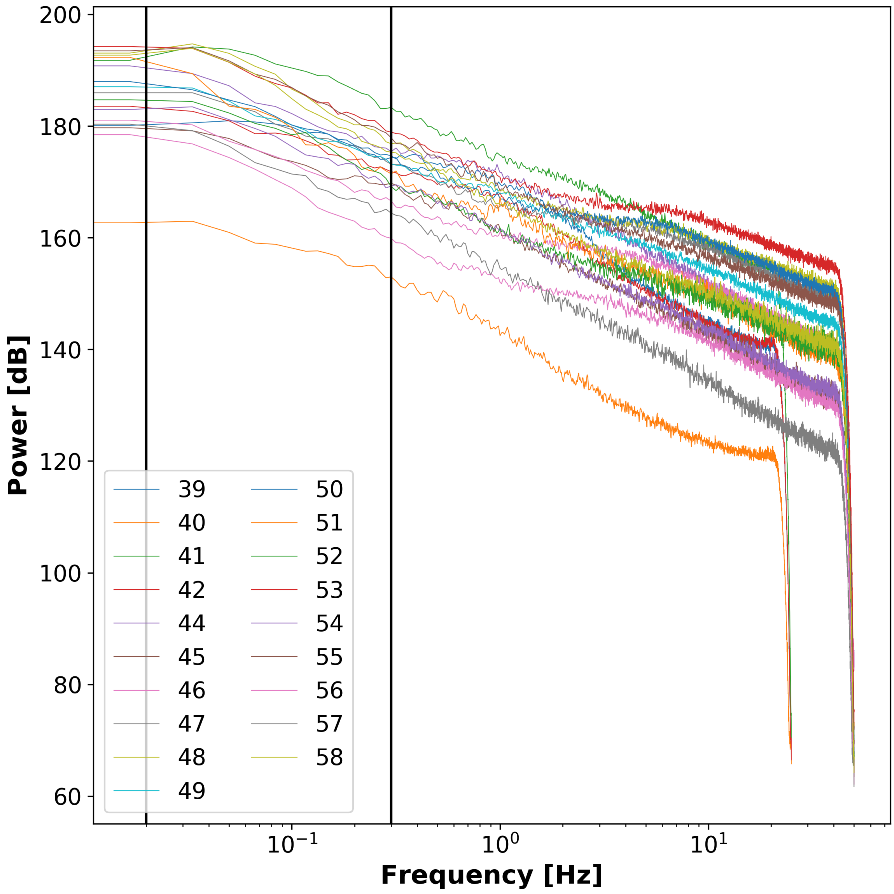

Figure S1. power spectral density (PSD) for the 60 minutes of CLES infrasound data prior to each explosion. The PSD uses 60 s windows with 50% overlap for the calculations, with vertical lines denoting the 0.02-0.3 Hz frequency band used as a proxy for wind noise in Fee and Garces (2007).

1.1.2 CLES/CLCO Seismic Amplitude Ratio

One method we used to investigate the potential changing source depth within the conduit is by taking the ratio of the peak amplitudes of the closer station (CLES) and the surface waves of the distal station (CLCO). This type of analysis draws similarities to the basis of the comparison of body-wave magnitude (M_b) and surface wave magnitude (M_s) for earthquakes (Båth, 1985). Higher values of the ratio may mean relatively more body wave/less Rayleigh wave. If a higher ratio were to correlate with higher positive traveltime residuals, then it may suggest deeper sources that generate less surface wave energy and have longer propagation in the conduit leading to the higher positive values of traveltime residual. Due to the lack of strong correlation and the reliance on a second seismometer, we do not include this analysis in the main paper. We note that this method may be useful for other seismometer configurations at other volcanoes.

We bandpass the displacement data between 0.25-0.5 Hz for both stations CLES and CLCO. Then, we find the peak amplitude of the p-wave within a window of 1.5 seconds after the onset on the East component (essentially the first positive bump). Similarly, we find the peak amplitude of the Rayleigh wave in the window of 5 seconds after the surface wave onset on the east component of station CLCO (positive, negative, positive bumps). Then, we divide the peak amplitude value of CLES by the peak amplitude value of CLCO for each explosion. A very weak to no correlation is found between this amplitude ratio and both the seismo-acoustic time lag and the travel time residual (R-squared values of 0.06 and 0.01, respectively, Figure S2a,b). We show the vertical and radial components of CLCO data, highlighting the Rayleigh wave with characteristic 90 degree phase shift for example Explosion 44 in Figure S2c,d.

REFERENCES

Båth, M. (1985). Surface-wave magnitude corrections for intermediate and deep earthquakes. *Physics of the Earth and Planetary Interiors* 37, 228–234. doi:10.1016/0031-9201(85)90010-X

Fee, D. and Garces, M. (2007). Infrasonic tremor in the diffraction zone. *Geophysical Research Letters* 34. doi:10.1029/2007GL030616

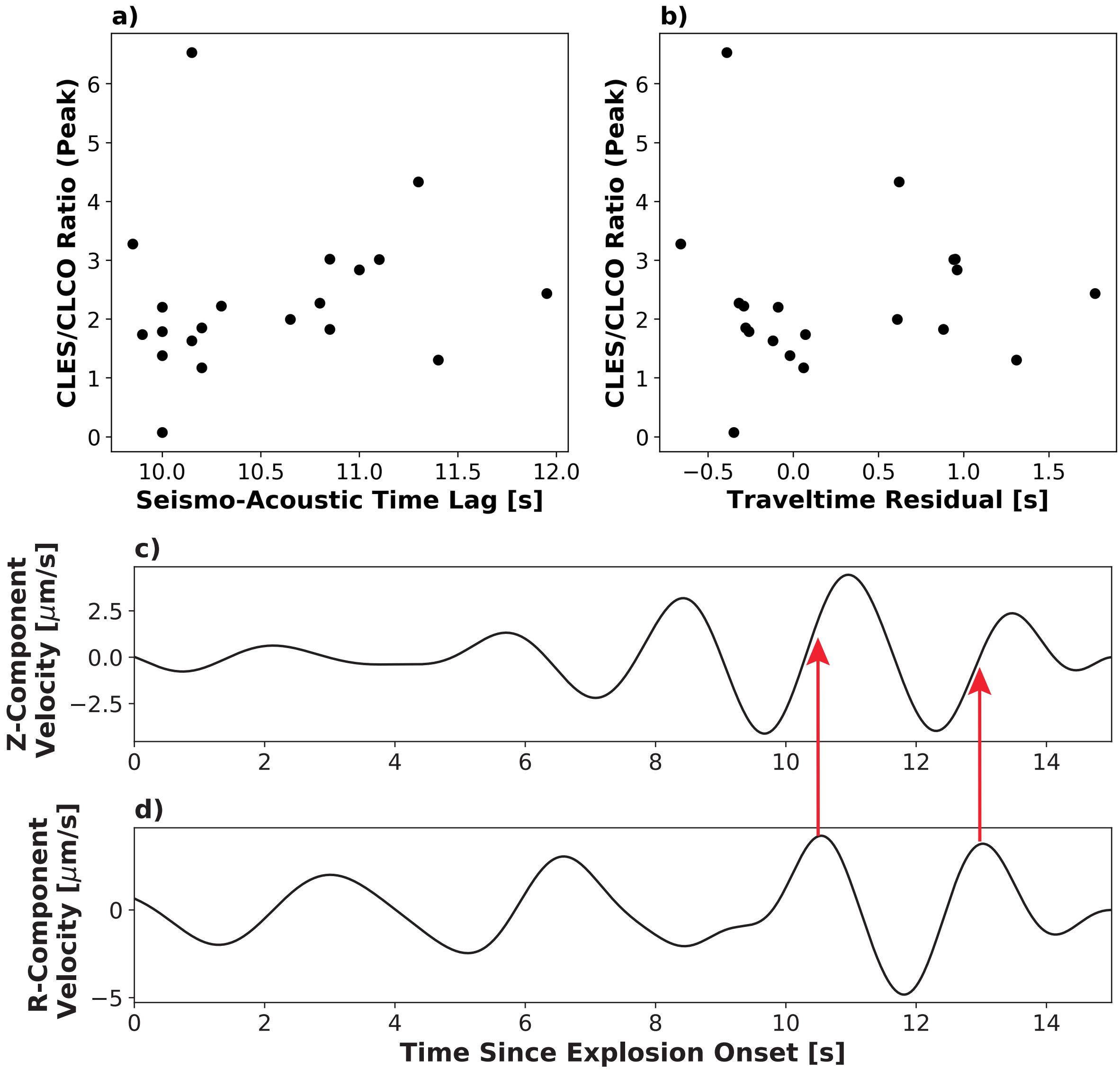

Figure S2. Peak amplitude ratio in the 0.25 - 0.5 Hz range between CLES and CLCO. Amplitude ratio consists of the peak displacement on the east component of the 1.5 s surrounding the p-wave on CLES and the 5 s surrounding the onset of the Rayleigh wave on CLCO. The amplitude ratio is plotted against **(a)** the seismo-acoustic time lag and **(b)** the travel time residual, showing little to no correlation. The **(c)** vertical and **(d)** radial components of the CLCO data show the Rayleigh wave with 90 degree phase shift, as highlighted by the red arrows.